

method for predicting yields of field desorption ion sources, to compute binding energies on individual crystal planes from measured desorption fields and to prepare the operation of a microsecond pulsed ion desorption microscope promising sufficient resolution to resolve the lattice structure of the emitting surface.

## ACKNOWLEDGMENTS

Thanks are due to Dr. R. H. Good, Jr., for discussions of the subject. The author appreciates further the assistance of Dr. K. Bahadur, D. W. Feldman, W. T. Pimbley, and R. D. Young in the experimental part of this work.

## Field Ionization of Gases at a Metal Surface and the Resolution of the Field Ion Microscope\*

ERWIN W. MÜLLER AND KANWAR BAHADUR†

*Field Emission Laboratory, The Pennsylvania State University, University Park, Pennsylvania*

(Received September 12, 1955)

The mechanism of field emission of positive ions is considered as depending upon the supply of molecules and their ionization probability in a field up to 500 million volts/cm. Experimental current-field characteristics match the theoretical curves. The velocity distribution, measured in a retarding potential tube, shows that the ions originate some 5 to 100 Å above the surface, depending upon the field. A simple mass spectrometer is described which uses the field emitter as a point ion source. The resolution of the field ion microscope is found to depend upon tip radius, polarizability and ionization potential of the gas, and possibly upon the accommodation coefficient and the temperature. Helium seems to give the best resolution of about 4 Å. The possibility of operating a field desorption microscope with sufficient resolution to show the lattice structure of the surface is discussed.

### 1. INTRODUCTION

A SUFFICIENTLY strong electric field applied to a metal surface in such a direction as to make the metal positive gives an emission of positive ions. If the ions originate in an adsorbed layer or are provided by the emitter material itself, the ion source will be weak and rapidly exhausted.<sup>1</sup> A steady ion current up to the microampere range can be obtained when the matter to be ionized is supplied from the gaseous phase. This kind of emission was first used in the field ion microscope,<sup>2</sup> which is a conventional field emission microscope<sup>3</sup> operated with reversed polarity and filled with a gas at a pressure of several microns. The field ion microscope promises to become a useful tool for the study of the structure and behavior of metal surfaces on an atomic scale.<sup>4</sup> However, so far only a few experiments with gases, other than the originally proposed hydrogen and helium, have been reported,<sup>5</sup> as well as the application of the hydrogen-ion microscope for the visualization of surface structures that were interpreted to be screw dislocations.<sup>6</sup> A suggestion about the mechanism of

field desorption has been made by Kirchner.<sup>7</sup> An important advance was made by Inghram and Gomer<sup>8</sup> when they introduced mass spectroscopical analysis of the field ions. Most of the results of the present paper were reported a year ago by one of the authors,<sup>9</sup> and a brief account of the subject is given in the *Encyclopedia of Physics*.<sup>10</sup>

### 2. THE SUPPLY FUNCTION FOR A POINT EMITTER

The ion current is the product of the number of gas molecules arriving at the emitter per unit of time, which we may call the supply function  $Z$ , and the efficiency of surface ionization. The number of molecules  $Z$  striking the tip is largely determined by the attraction of the molecules through the dipoles induced by the inhomogeneous field. We define a sphere of capture with radius  $r_c$  extending as far as the point where the dipole attraction is larger than or equal to the centrifugal force of a tangentially approaching molecule of polarizability  $\alpha$ :

$$-\alpha F dF/dr = mv^2/r_c. \quad (1)$$

We set  $mv^2/2 = kT$  and describe the field in the neighborhood of the tip by the semiempirical formula

$$F = 7.75 V r_0^{2/3} / r^{4/3}, \quad (2)$$

<sup>7</sup> F. Kirchner, *Naturwiss.* **41**, 136 (1954).

<sup>8</sup> M. Inghram and R. Gomer, *J. Chem. Phys.* **22**, 1279 (1954).

<sup>9</sup> E. W. Müller, *Field Emission Symposium*, Pittsburgh, 1954 (unpublished).

<sup>10</sup> R. H. Good, Jr., and E. W. Müller, review article on "Field Emission," *Encyclopedia of Physics* (new edition of *Handbuch der Physik*, Verlag Julius Springer, Berlin, to be published), Vol. 21.

\* This research was supported by the U. S. Air Force through the Office of Scientific Research of the Air Research and Development Command.

† On leave of absence from National Physical Laboratory of India, New Delhi.

<sup>1</sup> E. W. Müller, preceding paper [*Phys. Rev.* **102**, 618 (1956)].

<sup>2</sup> E. W. Müller, *Z. Physik* **136**, 131 (1951).

<sup>3</sup> E. W. Müller, *Z. Physik* **106**, 1 (1937).

<sup>4</sup> E. W. Müller, *Ergeb. exak. Naturw.* **27**, 290 (1953).

<sup>5</sup> M. Drechsler and G. Pankow, *Proceedings of the Conference on Electron Microscopy*, London, 1955.

<sup>6</sup> Drechsler, Pankow, and Vanselow, *Z. physik. Chem.* **4**, 249 (1955).

where  $V$  is the voltage applied between the tip and a distant negative electrode (e.g., the screen in the field ion microscope),  $r_0$  the tip radius in cm,  $F$  the field in esu/cm. This gives

$$r_c = 4\alpha^{3/8} V^{3/4} r_0^{1/2} / k^{3/8} T^{3/8}. \quad (3)$$

Assuming that outside the sphere of capture the molecules move as in an ordinary gas of pressure  $p$ , we obtain immediately the supply function  $Z$ , which equals the number of gas molecules striking the surface of the sphere of capture per unit of time. The fact that the tip is not a freely suspended sphere but resembles something between a hyperboloid and a sphere on a cone is neglected here, but not in Eq. (2).

$$Z = \frac{p}{(2\pi mkT)^{1/2}} \cdot 4\pi r_c^2, \quad (4)$$

$$Z = \frac{80p\alpha^{3/4} V^{3/2} r_0}{m^{1/2} k^{5/4} T^{5/4}}. \quad (5)$$

If all molecules striking the tip were ionized, the field ion current would be obtained by multiplying  $Z$  by the ion charge  $e$ . The result is in good agreement with the measured characteristics if we consider the high field range, where the ionization efficiency is unity. The  $\log I$  versus  $F$  characteristics in Fig. 1 have been taken at room temperature in two field ion microscope tubes with tip radii of 450 Å and 1000 Å. The current was found to be proportional to the pressure, which was varied from  $0.1\mu$  to about  $6\mu$  and in the case of helium up to  $25\mu$ . The currents in Fig. 1 are about 5 to 8 times larger than expected. This might be partly due to the imperfection of the theoretical treatment, but at least a factor of 3 should be ascribed to the presence of secondary electrons in the measured current. It is planned to eliminate the secondaries by using a special ion collector with a suppressor grid. For a given field at the tip surface,  $V^{3,2}$  is proportional to  $r_0$ , according to Eq. (2); so that the ion current in the high-field region should be proportional to  $r_0^2$  according to Eq. (5). Actually, the measured total currents depend on about the third power of tip radius. This is partly due to a larger fraction of secondary electrons at the higher voltages that are required to produce the same field for larger tip radii. For our calculations below, we have used the empirical formula  $\gamma = 4 \times 10^{-4} V$  for argon and  $2 \times 10^{-4} V$  for helium ( $V$  in volts) for the number of secondary electrons released by one ion.

### 3. EFFICIENCY OF FIELD IONIZATION AT A SURFACE

The shape of the ion current versus field strength characteristic at lower fields is mainly determined by the efficiency of surface ionization. In the high-field region, the potential wall surrounding the molecule is so narrow at the side towards the tip that electrons may tunnel out at a distance up to the order of  $r_0$  above the

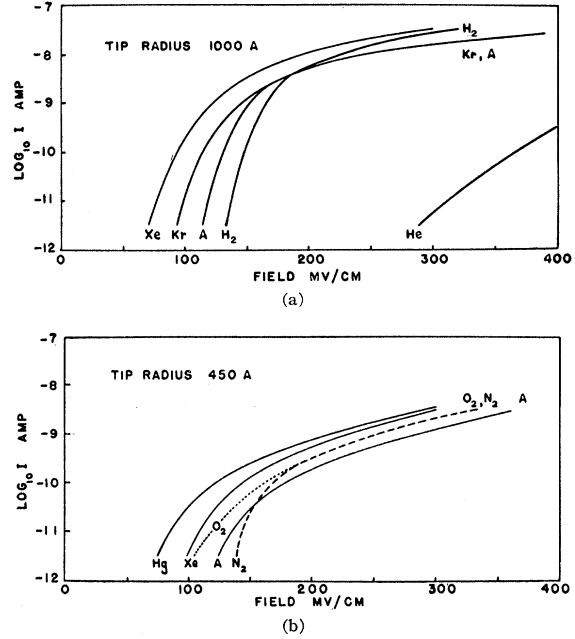


Fig. 1. Logarithm of current versus field strength characteristics measured in two field ion microscope tubes, with different tip radii. Gas pressure 1 micron.

tip surface. However, at a slightly smaller field, auto-ionization in space will be negligible. When the molecule approaches the surface of the tip very closely, the image potential provides an additional reduction of the potential wall. A numerical computation was carried out to determine the probability  $P$  that an electron tunnels while the atom approaches from a distance  $l$  to  $l-1$  Å with a speed determined by the attraction of the induced dipole. The efficiency of ionization will then be  $\int_0^\infty P dl$ . The potential effective on the electron at a distance  $x$  from the surface and along a line perpendicular to the surface and through the ion is assumed to be

$$V(x) = -\frac{e}{|l-x|-a} + Fx - \frac{e}{4x} + \frac{e}{l+x-a}, \quad (6)$$

where the first term represents the potential funnel of the ion ( $a$  is the ion radius) and the second one the external field; the third term is the image potential of the electron, and the fourth term describes the repulsion of the electron by the image of the ion in the metal. The wave mechanical penetration probability of the potential barrier, simplified to a linear problem, can be written as

$$D(l) = \exp \left[ -\frac{(8em)^{1/2}}{\hbar} \int_{x_1}^{x_2} \times \left( V(x) - Fl + V_I - \frac{e}{4l} \right)^{1/2} dx \right], \quad (7)$$

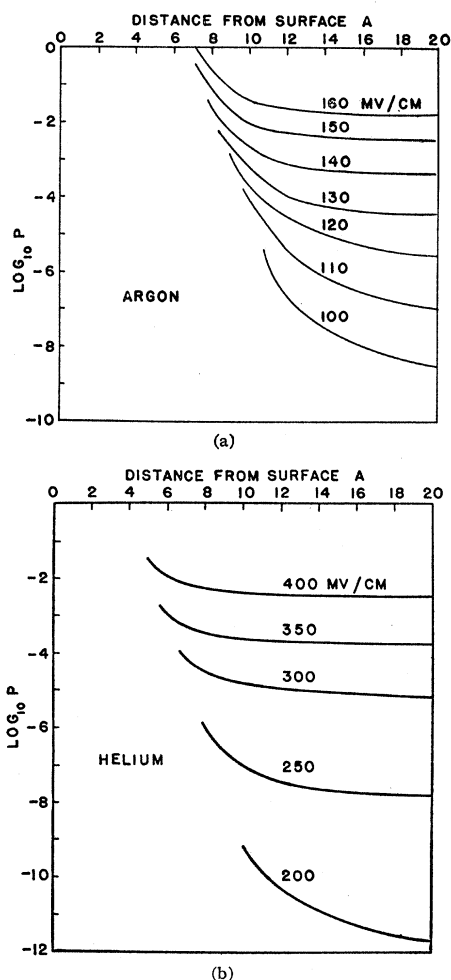


FIG. 2. Logarithm of probability  $P$  for an argon atom (a) and for a helium atom (b) to be ionized while traveling from  $l$  to  $l-1$  Å toward the tip surface with a velocity determined by the dipole attraction.

where  $V_I$  is the ionization potential.  $D(l)$  was calculated by graphical integration. The transition from the linear problem to the actual spatial penetration probability can be achieved, making a rather crude approximation, by assuming the corresponding integral through the potential at angle  $\varphi$  with the normal to be proportional to  $1/\cos\varphi$ . Then averaging over  $\varphi$  (only small angles are important) gives

$$\Delta(l) = -D(l)/\ln D(l) \quad (8)$$

for the whole transparency of the potential hump. The ionization probability  $P$  is finally obtained by multiplying  $\Delta(l)$  by the frequency  $\nu$  with which an electron strikes the inner wall of the potential funnel ( $\nu = 1.5 \times 10^{16} \text{ sec}^{-1}$  for argon and  $2.4 \times 10^{16} \text{ sec}^{-1}$  for helium; these numbers are found from the Bohr orbit picture using Finkelburg's<sup>11</sup> values for the effective nuclear

<sup>11</sup> W. Finkelburg, *Atomic Physics* (McGraw-Hill Book Company, Inc., New York, 1950), p. 172.

charge) and by the transit time  $m^3/F\alpha^3$  required for the molecule to move through the distance of one Å in approaching with the radial velocity determined by the dipole attraction only.

The result of this computation is presented in Figs. 2(a) and 2(b). The ionization probability curve of the approaching atom ends suddenly at a certain minimum distance  $l_{\min}$  from the surface when the ground level sinks below the Fermi level inside the metal; past this point an electron can no longer find an unoccupied level. The ion current produced by the atoms during their approach to the tip is then obtained by integrating the probability  $P$  from  $l_{\min}$  to infinity and multiplying it by the ion charge and the supply function.

The actual ion current is larger because the molecules that have not been ionized while approaching will be reflected from the surface and pass in the reverse direction through the zone of high ionization probability close to the surface and beyond the Fermi level barrier. This time the ionization probability will be larger than while approaching the tip. While the approaching molecule moves almost perpendicularly to the surface, as long as the dipole attraction energy component  $\frac{1}{2}\alpha F^2$  is essentially larger than  $kT$ , the reflected molecule may have any random direction and a lower average velocity corresponding more or less to the tip temperature, depending on the accommodation coefficient of the gas-surface combination. On the average the reflected molecule will therefore stay much longer in the zone of high ionization probability. Assuming a small accommodation coefficient and random reflection, one finds the average normal rebound velocity to be half the incident velocity. Therefore the total ion current will be

$$I^+ = 3eZ \int_{l_{\min}}^{\infty} P dl. \quad (9)$$

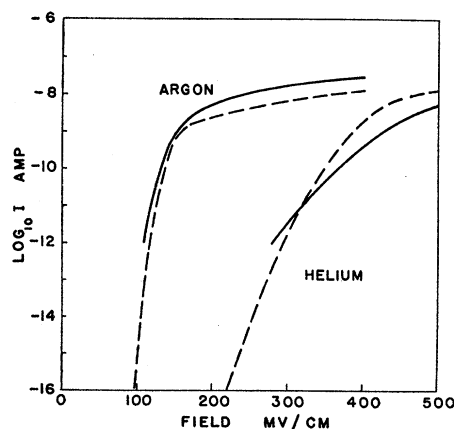


FIG. 3. Theoretical current-field characteristics (dashed line) computed from Eq. (9) for one micron gas pressure and 1000 Å tip radius, in comparison with experimental curves (solid line).

The total currents actually measured in a field ion microscope (Fig. 1) are expected to be larger by a factor  $\gamma+1$  due to  $\gamma$  secondary electrons released by each ion at the screen and the other negative electrodes. The integral in Eq. (9) has been evaluated numerically for argon and helium, using the field distribution of Eq. (2). The result, given as theoretical ion current *versus* field strength characteristic in Fig. 3, agrees well enough with the experimental curves in Fig. 1 to support our ionization mechanism. A too close agreement cannot be expected, not only because of the present uncertainties in field determination and the effect of secondary electrons, but also because the calculations are sensitive to the rather crude assumption for the shape of the potential funnel in Eq. (6).

There is no sharply defined minimum field strength for field ion emission. For different gases one finds experimentally (Fig. 1) the field for the onset of the current to be closely proportional to the  $\frac{3}{2}$  power of the ionization potential. This further confirms our mechanism, since approximating the integrand of Eq. (7) by a right angle triangle with altitude  $V_I$  and with the slope of its hypotenuse proportional to the field, one finds the integral proportional to  $V_I^{3/2}/F$ , which should be about the same for all gases under the onset conditions.

Experiments to check the assumption of the significance of the rebound molecules have been made by varying gas temperature and tip temperature independently. As expected, in the low-field range of the characteristic the ion current decreases considerably with increasing tip temperature, while the current increases when the whole tube is immersed into liquid air.

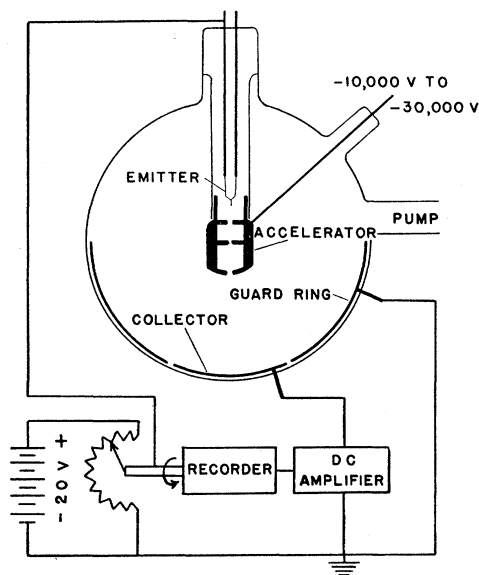


Fig. 4. Retarding potential tube for measuring energy distribution of field ions.

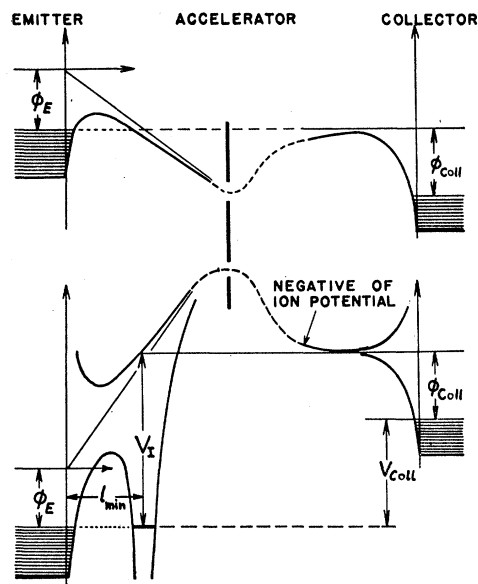


Fig. 5. Potential diagram for retarding potential tube, above for negative emitter (electron emission) and below for positive emitter (ion emission). Compared with the field at the emitter, the field at the collector is actually much smaller than shown here.

#### 4. VELOCITY DISTRIBUTION OF FIELD ION EMISSION

The origin of the ions can be localized by measuring their velocity distribution. Only those coming directly from the surface will finally have the full velocity corresponding to the voltage applied to the accelerating electrode, while those produced at a certain distance from the tip will have less velocity. Inghram and Gomer<sup>8</sup> have reported measurements of peak widths as obtained in a precision mass spectrometer. Although the resolution of 20 volts limits the accuracy, the broadening of the peak width with increasing field indicates clearly that at least some ions are produced at a distance from the tip.

In the course of our work we have used the retarding potential method, which has already proved to be reliable for measuring the velocity distribution of field electron emission within an accuracy of a few hundredths of a volt. The tube illustrated in Fig. 4 is first used to measure field electron emission in order to obtain the work function of the collector  $\phi_{coll}$ . It equals the voltage at which electrons start to enter the collector according to potential diagram Fig. 5. Field ions produced, after about 0.1 micron of gas has been admitted and after the voltages have been reversed, can reach the collector only if it is negative by  $V_{coll} = V_I - \phi_{coll}$ . Figure 6 gives recorded collector currents as a function of the collector voltage. Actually the observed current has the direction of entering electrons. These are produced when the ions that cannot reach the collector fall back and strike the outside surface of the accelerating electrode and also when collisions occur in the gas. The total current begins to drop when ions

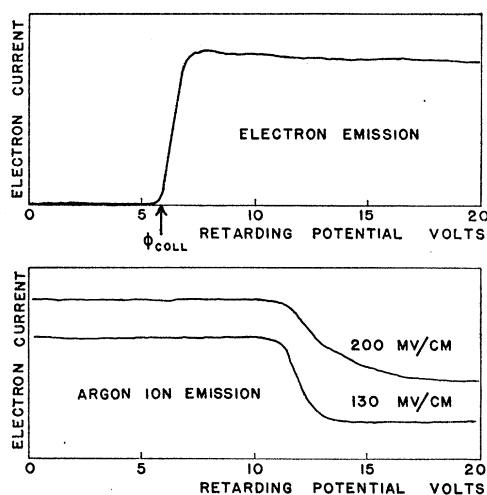


FIG. 6. Recorded collector currents of retarding potential tube. The currents are of the order of  $10^{-12}$  amp. Differentiation gives a half-width of 1.0 ev at 130 MV/cm and of 3.1 ev at 200 MV/cm for the energy distribution of the argon ions. The half-width of the electron emission energy distribution is 0.43 ev.

start contacting the collector. For argon the onset of ion current is at 10 volts, exactly where it should happen according to our potential diagram, since  $\phi_{coll} = 5.7$  ev and  $V_I = 15.7$  ev. In the same way, the onset for xenon is found at 6.5 volts and for helium at 19 volts. Differentiation of the voltage-current recordings gives the energy distribution, which shows clearly the origin of the ions beyond the expected minimum distance from the surface. At higher fields, where auto-ionization in space becomes effective, the distribution curve is much wider. The distribution width can be calculated from  $\int Pdl$  and there is complete agreement with the experimental result derived from Fig. 6 for argon.

##### 5. THE FIELD ION EMITTER AS AN ION SOURCE

The value of the field ion emitter as an ion source for a mass spectrometer has already been emphasized by Inghram and Gomer.<sup>8</sup> They modified the field ion microscope by the introduction of a small hole in the screen through which an ion beam passed into a mass spectrometer equipped with an electron multiplier as the ion detector. The most remarkable property of the field ion emitter compared to conventional ion sources is the fact that in the high-field range the ions are produced before the molecules contact the tip surface, and that no hot filaments are present. This results in a negligible fragmentation of molecules and offers great advantages in mass-spectroscopical analysis. Another valuable property of the field ion emitter is the small size of the emitting region, which makes it practically a point source with ion current densities up to above 100 amp/cm<sup>2</sup>. This allows the source itself to be used as an entrance slit of the spectrometer. Figure 7 shows a design of a mass spectrometer in which the point

source is focused on a fluorescent screen by a three-element electrostatic lens. Because of the small magnification, about 20 times, and a desired image spot diameter of 0.2 mm, the numerical aperture of the lens could be made as large as about 0.2, so that a large fraction of the total ion current is utilized. In this experimental tube which was designed mainly to study the mechanism of field ionization of molecular gases, a resolution of about 80 was obtained with a 20-lb magnet, enough to just resolve the krypton isotopes. Intensities can be measured photometrically on the screen. The wide aperture of the lens makes it difficult to maintain a very high vacuum in the deflection chamber, so that at larger pressures the image points on the screen show tails produced by charge exchange during gas collisions. Results obtained with this mass spectrometer will be reported in another publication.

##### 6. THE RESOLUTION OF THE FIELD ION MICROSCOPE

Field ionization at a surface was discovered when a conventional field electron microscope was operated with reversed polarity in hydrogen<sup>2</sup> for the purpose of obtaining an improved resolution. This field ion microscope was then thought to utilize field desorption directly from the surface. However, the failure to obtain improved resolution at liquid air temperature, with hydrogen ions as well as with argon ions, and further the steady transition of a sharp image to a blurred one at increasing fields, suggested that the ionization occurs in space above the surface, as discussed in the foregoing paragraphs. Nevertheless, the basic principles for treating the resolution of the field electron microscope, as developed by Benjamin and

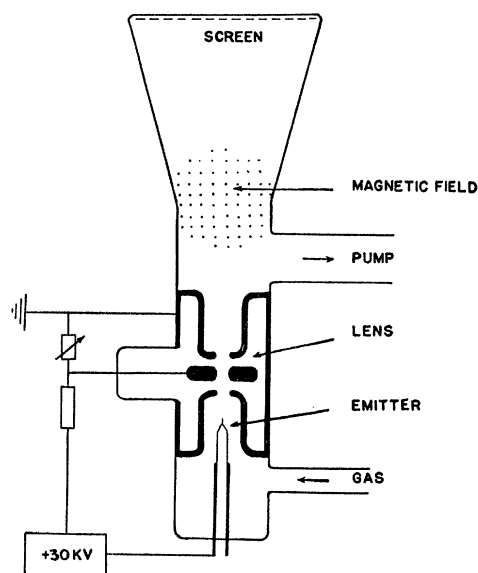


FIG. 7. Mass spectrometer tube.

Jenkins<sup>12</sup> and by Müller,<sup>13</sup> which were discussed again with more detail by Ashworth<sup>14</sup> and Gomer,<sup>15</sup> can be applied to the ion microscope as well.

Three factors determine the size of the image of an object on the tip: The divergence of the ion orbits due to the magnification of the tube by straightforward central projection, the velocity component of the ions parallel to the tip surface, and finally the diffraction due to the wave nature of the ions, which can be described as well by the Heisenberg uncertainty principle.

The magnification of a field emission microscope is

$$M = R/\beta r_0, \quad (10)$$

where  $R$  is the distance from the tip to the screen,  $r_0$  the tip radius, and  $\beta$  an "image compression factor," which takes into account that the emitter is not a freely suspended sphere, but is supported by the conical shank. The factor  $\beta$  equals about 1.5 and can be measured accurately in the crystal pattern of a given tip. The minimum image size  $\Delta_{\min}$  is given<sup>10</sup> by

$$\Delta_{\min}^2 = 2\hbar\tau M/m + 4\bar{v}_y^2\tau^2, \quad (11)$$

where the first term describes the effect of the uncertainty and the magnification, the second one the image broadening by the average tangential velocity component  $\bar{v}_y$ . Here  $\tau$  is the time of flight of the ion, which is very close to  $R \times (m/2eV)^{1/2}$ . Dividing Eq. (11) by the magnification, one obtains the object side resolution:

$$\delta = \left( \frac{2\hbar\beta r_0}{(2emV)^{1/2}} + \frac{2\beta^2 r_0^2 m \bar{v}_y^2}{eV} \right)^{1/2}. \quad (12)$$

For ions the first term, representing the square of the magnification-diffraction contribution, is at least 100 times smaller than for electrons and is thus practically negligible. The second term will also be smaller, because of the higher voltage, if the transverse energy component  $\frac{1}{2}m\bar{v}_y^2$  is of the same size as for electrons. Because of the radial field, the approaching gas molecules will have no more average tangential energy than  $kT$ , which at room temperature is already about 4 times smaller than the corresponding energy of field electrons, and could easily be decreased by operating the ion microscope at lower temperatures. Unfortunately, as has been made evident in Sec. 3, most of the ionization occurs when the gas molecules are rebounding from the surface. They will have a randomly directed velocity with an average kinetic energy up to  $m\bar{v}^2/2 = \frac{3}{2}kT + \frac{1}{2}\alpha F^2$ , which results in a resolution

$$\delta = \left( \frac{2\hbar\beta r_0}{(2emV)^{1/2}} + \frac{\pi^2\beta^2 r_0^2 (3kT + \alpha F^2)}{8eV} \right)^{1/2}. \quad (13)$$

<sup>12</sup> M. Benjamin and R. O. Jenkins, Proc. Roy. Soc. London **A176**, 262 (1940).

<sup>13</sup> E. W. Müller, Z. Physik **120**, 270 (1943).

<sup>14</sup> F. Ashworth, Advances in Electronics **3**, 1 (1951).

<sup>15</sup> R. Gomer, J. Chem. Phys. **20**, 1772 (1952).

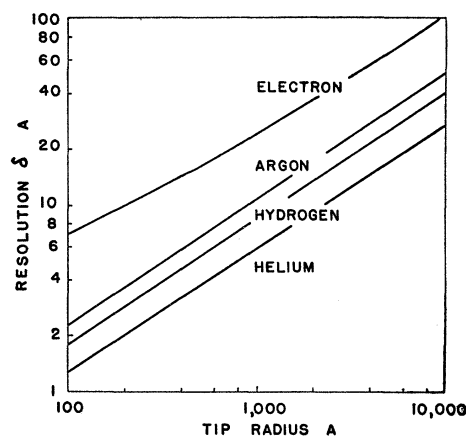


FIG. 8. Theoretical resolution of the field emission microscope, for electrons and for helium, hydrogen, and argon ions.

The energy term due to the dipole attraction  $\frac{1}{2}\alpha F^2$  is, in the practical field range, usually larger than the thermal energy at room temperature, for instance 0.1 eV for He at 375 Mv/cm and 0.22 eV for A at 200 Mv/cm. Since it shows up as a tangential component only after reflection at the surface, one can hope to eliminate its disturbing effect by providing a gas-surface combination with an accommodation coefficient close to unity. Unfortunately, the accommodation coefficient for helium on clean tungsten is rather small. However, at a sufficiently low temperature, perhaps below liquid air temperature, it should increase. It appears also that the more detailed images which one obtains from an oxygen-covered tungsten tip could be ascribed to an increased accommodation coefficient.

With the significance of the polarizability in Eq. (13), we can assume that helium with its extremely small  $\alpha$  is a most suitable gas for an ion microscope.<sup>16</sup> In Fig. 8 the resolution of ion microscopes has been calculated in the case of He for a field of 350 Mv/cm and in the cases of A and H<sub>2</sub> for a field of 180 Mv/cm, which seems to be about optimum. For comparison the resolution of the field electron microscope, with a typical operation range of 35 to 50 Mv/cm, has also been calculated, using Eq. (12) and an average tangential energy component<sup>4</sup> of  $\epsilon_y = 0.67 \times 10^{-8} F \phi_E^{-1/2}$  ( $\epsilon_y$  and  $\phi_E$  in eV, and  $F$  in volts/cm).

Actually, we should rather call the result of Eq. (13) the potential resolution, since it is the resolution obtainable in the region where the ions originate, parallel to and about 5 to 10 Å above the surface. No more detail can appear in the image than that which is contained in the local potential profile between the border of the ionization zone at  $l_{\min} \approx (V_I - \phi_E)/F$  and the actual surface. Edges of single lattice steps should certainly show up in the potential profile at that distance, but the fine field ripple produced by the individual atoms might be too small to give sufficient

<sup>16</sup> E. W. Müller, Deutsches Patent No. 868 030 (1951).

intensity variation. It seems to be important to choose the applied field according to Fig. 2. At low fields the contrast is better, but the ions originate too far from the surface. Too high fields, on the other hand, will produce too much autoionization before the molecules approach the surface close enough for encountering sufficient differentiation in the local field. Evaluating  $\int Pdl$ , one finds for instance that for He at 400 Mv/cm half of the ions originate in a distance between 5 and 21 Å from the surface, and 10% originate only 5 to 5.7 Å above the surface, yielding a high-resolution image with low contrast.

Considering the difficulties in evaluating the potential profile above an atomically rough surface, one can say that the experiments confirm fully the expectations about the resolution. Using the noble gases, and hydrogen, nitrogen, oxygen, and mercury, one finds by far the finest details in the helium-ion image of a tungsten tip. While all the other gases gave a gaseous discharge breakdown at pressures above 5 to 10 microns, helium microscopes could be operated up to pressures of 50 microns, but with some loss of definition due to scattering of the ions in the gas. This high pressure helps a little to balance the extremely small intensity obtainable with helium because of the small dipole capture. For best resolution, very fine tip radii were used; this decreased the intensity again. Usually the tips were sharpened in the tube itself by the old methods of cathode sputtering<sup>17</sup> or oxide evaporation,<sup>18</sup> and finished by field evaporation.<sup>1</sup> The determination of the tip radius and hence the magnification by measuring field electron emission is rather difficult, since the removal of an oxygen film can be achieved only by field evaporation at room temperature. Heating the finished tip to the evaporation temperature of an oxygen film, above 2000°K, would immediately increase the tip radius

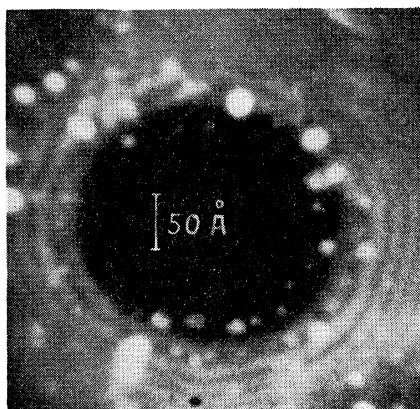


FIG. 9. Helium-ion image of the center of a tungsten tip, with individual lattice steps around the 011 plane. Tip radius  $r_0=1000$  Å. Helium pressure 15 microns. Voltage 23 000 volts corresponding to  $F=380$  Mv/cm.

<sup>17</sup> E. W. Müller, *Z. Physik* **106**, 132 (1937).

<sup>18</sup> E. W. Müller, *Z. Physik* **108**, 668 (1938).

beyond the desired size. We assume that the data given for the tip radii in Figs. 9 to 11 are correct within about  $\pm 25\%$ . Figure 9 shows the center of the pattern of a tungsten tip, the dark area being the 011 plane, surrounded by individual lattice steps. On the original photograph about 9 to 10 concentric rings can be counted, which occupy a region with a maximal apex angle  $\vartheta$  of about  $13^\circ$  (almost half the way to the 112 plane, for which  $\vartheta=30^\circ$ ). The cap of a sphere with this apex angle and a radius of 1000 Å is 25 Å high, which is pretty close to 10 layers of 011 planes (2.35 Å each). We conclude that this fine tip had an almost spherical shape, and that the individual lattice steps were resolved. The spacing of these steps can be calculated from the lattice structure. On the right side of the picture, the 122 plane with a spacing of 6.7 Å is clearly resolved. The ion image provides a perfect topographic

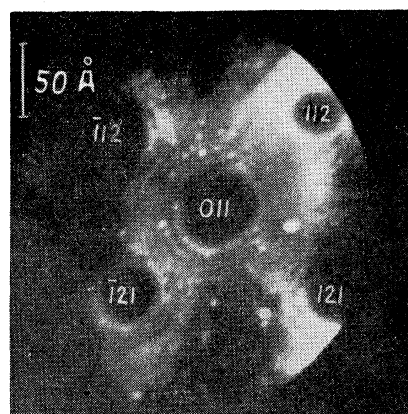


FIG. 10. Helium-ion image of a tungsten tip with lattice steps around the 011 plane in the center. Tip sharpened by cathode sputtering, and smoothed by annealing at 950°K. Field electron emission of 1 microampere at 920 volts, corresponding to tip radius of about 200 Å. Ion image made with 25 microns of helium at 8900 volts corresponding to about 420 Mv/cm.

map of the emitter tip with the lattice steps as contours. This suggests an application of this map to obtain a more accurate field calibration for checking the Fowler-Nordheim theory of field electron emission more closely.

The tip radius in Fig. 10 is about 200 Å, resulting in a higher resolution. At least on the original photograph a pearl chain structure of the lattice steps in the region between the central 011 plane and the four surrounding dark 112 planes can be clearly recognized, where the spacing in the chain is 4.5 Å. This photograph required  $\frac{1}{2}$ -hour exposure with an  $f:1$  objective and Tri X film. The individual atoms constituting the lattice steps were better observed visually with the help of a special 15 times magnification microscope with numerical aperture 0.5 and coated lenses, and a perfect dark adaptation of the eye. During the long photographic exposure time, the fine details might easily undergo a change by adsorption, surface migration, and field desorption of contaminations in the helium, and at

fields above 450 Mv/cm by field desorption of tungsten itself.

Damage to the tip surface due to the impinging helium atoms is negligible, since at 450 Mv the kinetic energy of the dipoles is only 0.14 ev. Gaseous contaminations which all have larger polarizabilities than He cannot approach close to the tip because they are ionized at a large distance from the emitter, thus reducing only the contrast.

At a field of about 500 Mv/cm the ionization of helium occurs almost completely at a large distance from the tip by autoionization. However, some details of the tungsten surface still remain visible in an image of low contrast, showing the dissolution of the surface lattice planes by field evaporation at room temperature. Some experimental data in the preceding paper have been obtained this way. By lowering the field the momentary state of the surface can be frozen in and photographed. Figure 11 shows the 011 plane of a 1000 Å tip in a state where the central residual 011 plane was just stopped before total dissolution. While in motion the edges of the collapsing rings are seen to be disappearing in little steps, undoubtedly due to the removal of individual atoms. The lattice steps of dissolving planes, which can be observed on 011, 112, and 001 always form closed rings. No spiraling was ever observed on such surfaces. The situation might be different at high temperatures, where Drechsler, Pankow, and Vanselow<sup>6</sup> interpret their observations with the lower resolution and the lower field of a hydrogen-ion microscope as an effect of screw dislocations with step heights of 4.5 to 60 Å.

We also could not find a particularly high resolution with mercury ions, as is claimed by Drechsler and Pankow.<sup>5</sup> Although a very faint ion image appears at about 60 Mv/cm, the optimum field seems to be about 100 Mv/cm, for which the potential resolution, according to Eq. (13), is slightly less than for argon. However, because of the low ionization potential, the Fermi level limit of ionization lies as close as 6 Å above the surface, so that the potential resolution can be almost fully utilized. If the ion microscope were operated with Hg at a relatively low tip temperature, the accommodation coefficient might be one and the resolution could be about 2 times better than for argon. We had difficulties in observing Hg ion images from tips with sufficiently small radii because of the low intensity. At 1000 Å tip radius, the resolution seemed not to be better than 8 Å.

## 7. THE FIELD DESORPTION MICROSCOPE

The limitation in resolution due to the large tangential velocity component of the rebound molecules can be



FIG. 11. Helium-ion image of a 011 plane of a tungsten tip with 1000 Å radius, after 10-sec exposure to 500 Mv/cm. Dissolution of 011 lattice planes was halted by lowering the field to 375 Mv/cm, and the picture was taken at this field.

overcome either by working at a sufficiently low tip temperature<sup>10,19</sup> as to make the accommodation coefficient one, or by allowing the impinging molecules to sit on the surface until they have transferred their excess energy to the substrate and come off with an average tangential energy of  $kT$  only. This can be done by operating the field ion microscope with pulses rather than with dc. The repetition rate has to be chosen so that in the time between two pulses the tip is covered with a fraction of a monolayer of the gas, and the pulse voltage must be high enough to desorb the monolayer during the pulse time.<sup>1</sup> The ratio of pulse width to repetition time must be very small, perhaps 1/1000, in order to keep the intensity of the blurred background low, which is produced by autoionization far above the surface during the pulse time. Since the sticking probability of nitrogen molecules<sup>20</sup> striking a tungsten surface at room temperature is 0.5, as long as the coverage is less than  $2.5 \times 10^{14}$  atoms/cm<sup>2</sup>, one can build up and tear off about 1500 of such layers within one second, if nitrogen is applied at a pressure of one micron. So far, our experiments with microsecond pulses and a repetition rate of 1000 to 2000 per second did not yet give a satisfactory intensity in the image. The desorption field strength for nitrogen on tungsten is probably about 500 Mv/cm, and very close to the desorption field strength of tungsten itself. It might be, therefore, better to look for another gas for a field desorption microscope with maximal resolution.

The authors wish to express their appreciation to Dr. R. H. Good, Jr., for discussions on the subject of this paper and for reading the manuscript.

<sup>19</sup> E. W. Müller, Z. Naturforsch. 11a, 89 (1956), and J. Appl. Phys. 27, 474 (1956).

<sup>20</sup> J. A. Becker and C. D. Hartman, J. Phys. Chem. 57, 157 (1953).



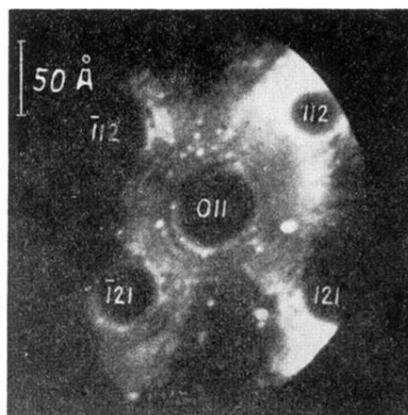


FIG. 10. Helium-ion image of a tungsten tip with lattice steps around the 011 plane in the center. Tip sharpened by cathode sputtering, and smoothed by annealing at 950°K. Field electron emission of 1 microampere at 920 volts, corresponding to tip radius of about 200 Å. Ion image made with 25 microns of helium at 8900 volts corresponding to about 420 Mv/cm.

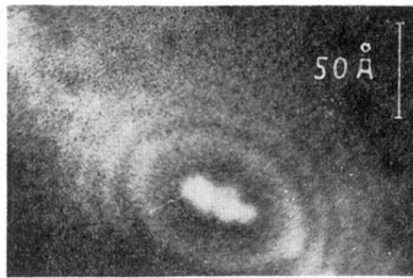


FIG. 11. Helium-ion image of a 011 plane of a tungsten tip with 1000 Å radius, after 10-sec exposure to 500 Mv/cm. Dissolution of 011 lattice planes was halted by lowering the field to 375 Mv/cm, and the picture was taken at this field.

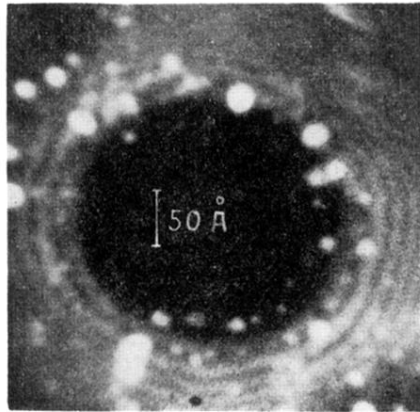


FIG. 9. Helium-ion image of the center of a tungsten tip, with individual lattice steps around the 011 plane. Tip radius  $r_0=1000$  Å. Helium pressure 15 microns. Voltage 23 000 volts corresponding to  $F=380$  Mv/cm.